Separation and Characterization of $C_{70}(C_{14}H_{10})$ and $C_{70}(C_5H_6)$ from an Acetylene–Benzene–Oxygen Flame

Qun-Hong Weng,[†] Qiao He,[†,‡] Di Sun,[†] Hui-Ying Huang,[§] Su-Yuan Xie,*[,†] Xin Lu,*[,†,‡] Rong-Bin Huang,[†] and Lan-Sun Zheng[†]

[†]State Key Laboratory of Physical Chemistry of Solid Surfaces and Department of Chemistry, College of Chemistry and Chemical Engineering, Xiamen University, Xiamen, 361005, China

[‡]Fujian Provincial Key Laboratory of Theoretical and Computational Chemistry, Xiamen University, Xiamen, 361005, China

[§]School of Life Science, Xiamen University, Xiamen, 361005, China

S Supporting Information

ABSTRACT: Although derivatives of fullerenes are prevalent in the fullerene-producing flame, the chemistry of these derivatives has rarely been discussed in the previous literature. In this paper, two D_{5h}-C_{70} derivatives, $C_{70}(C_{14}H_{10})$ and $C_{70}(C_5H_6)$, were isolated from the soot of an acetylene–benzene combustion. On the basis of detailed MS, NMR, IR, and UV/vis analyses in combination with DFT calculations, the cycloadduct structures of $C_{70}(C_{14}H_{10})$ and $C_{70}(C_5H_6)$ were identified. Both the anthracene ($C_{14}H_{10}$) and the cyclopentadiene (C_5H_6) adducts, supposed as the intermediate species produced during the combustion process, were characterized to bond at a [6,6] ring junction at the end of the olivary C_{70} cage. The present work exemplifies the capture of possible intermediates by the C_{70} fullerene from the flame and thus provides insight into the mechanism responsible for the formation of fullerene-containing soot.

Flame intermediates captured by fullerenes
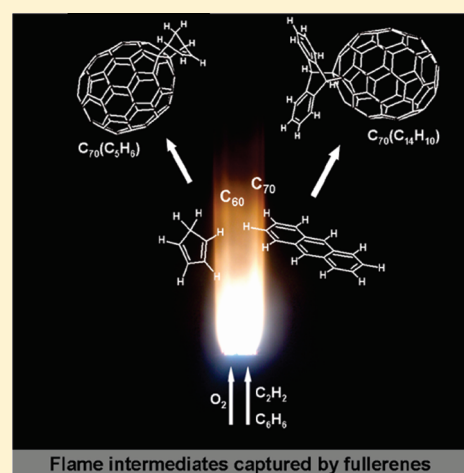
1. INTRODUCTION

Fullerenes can be macroscopically synthesized by various methods, such as arc-discharge,[1,2] combustion,[3-8] pyrolysis,[9-12] microwave plasma,[13,14] laser ablation,[15] glow discharge,[16,17] and traditional chemical synthetic methods.[18-21] Among them, the low-pressure incomplete combustion is applicable as an industrial method for fullerene production in ton scale.[8] However, the mechanism responsible for fullerene formation in a flame is still a puzzle to chemists and physicists. In the past two decades, a few interpretations have been proposed for understanding fullerene growth in the combustion process.[22-26] For example, polycyclic aromatic hydrocarbons (PAHs) were proposed as being the precursors of fullerenes in low-pressure flames in either a "zipper mechanism" or an "acetylene mechanism".[24,25] Special attention was paid to the smallest rings, such as C_5 (five-membered ring) and C_6 (six-membered ring), and their roles as nascent intermediates toward the formation of PAHs. Both C_5 and C_6 were supposed as the starting nuclei for sequential growth of larger PAHs via stepwise addition of C_2H_2 and loss of hydrogen atoms.[24,25] Both the optical spectroscopies (i.e., laser-induced fluorescence and coherent anti-Stokes Raman spectroscopy[27,28]) and the mass spectrometry (MS) were developed to experimentally probe possible intermediates involved in the combustion.

However, authentic structural identification of the intermediates in situ remains to be explored, even though intermediate ions or radicals in flames can be probed by MS if coupling with a molecular beam sampling technique and synchrotron photoionization.[26,29-32]

Inspired by the organic reactions of fullerenes with various radicals,[33] fullerenes have been applied as excellent radical scavengers,[34-36] with the implication of using flame-produced fullerenes as possible "sponges" to capture the intermediates formed in the combustion process. Accordingly, some of the intermediate species might be captured in the fullerene-producing flame as fullerene derivatives survivable in the ultimate products of combustion. Separation and characterization of these fullerene derivatives allows retrieval of the combustion intermediates, which, in turn, provides clues for mechanistic studies. Heretofore, only a C_{60} derivative, $C_{60}(C_5H_6)$,[37] has been previously separated and characterized among the products of combustion. The structures of other fullerene derivatives remain unknown, largely due to the difficulty in isolation and purification of these derivatives from the combustion products. In the present
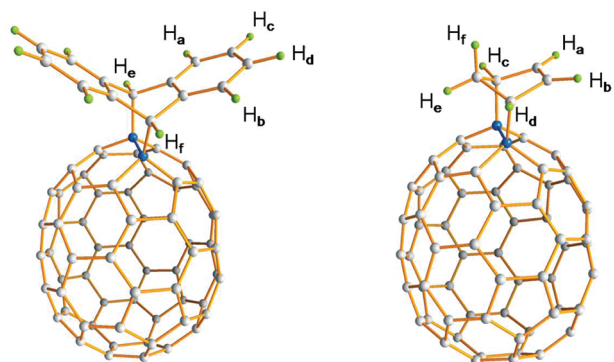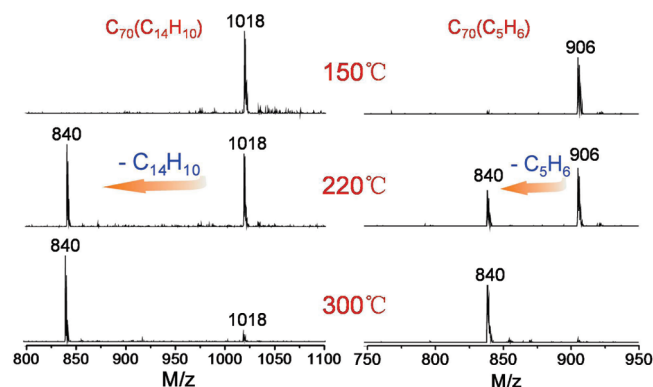
Figure 1. B3LYP/6-31G** level optimized structures of $C_{70}(C_{14}H_{10})$ (left) and $C_{70}(C_5H_6)$ (right).

Figure 3. Five types of carbon atoms and eight types of C—C bonds in C_{70}. The bond lengths are extracted from ref 46.

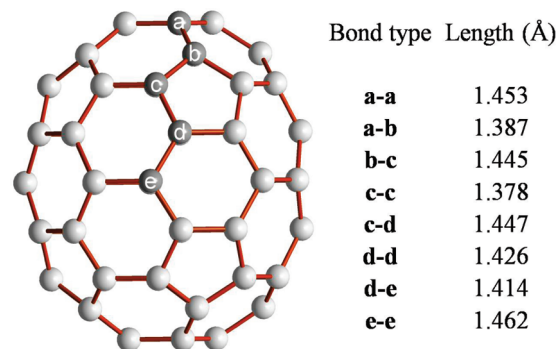| Bond type	Length (Å)
a-a	1.453
a-b	1.387
b-c	1.445
c-c	1.378
c-d	1.447
d-d	1.426
d-e	1.414
e-e	1.462

Figure 2. APCI-MS of $C_{70}(C_{14}H_{10})$ (left) and $C_{70}(C_5H_6)$ (right) in different ionization temperature conditions.

work, two C_{70} derivatives, $C_{70}(C_{14}H_{10})$ and $C_{70}(C_5H_6)$ (Figure 1), have been chromatographically separated from flame soot and characterized by MS, NMR, IR, and UV/vis analyses in combination with theoretical simulation. The identified structures of the C_{70} derivatives are informative for synthetic and mechanistic study.

2. EXPERIMENTAL SECTION

2.1. Synthesis of Fullerene Species in the Flame. The fullerene-producing diffusion flame was managed to be stabilized under a pressure of 15—20 Torr in a homemade setup, whose burner consists of two concentric tubes with 8 and 16 mm inside diameters with oxygen flowing in the inner tube.[38] The mixtures of acetylene, vaporous benzene, and oxygen were burned with the flow rates of 0.55, 1.0—1.1, and 1.1 L/min, respectively. Under such optimal conditions, the fullerene-containing soot productivity can reach up to 5 g/h. About 500 g of soot was collected for further HPLC separation and purification for fullerene derivatives.

2.2. HPLC Separation of $C_{70}(C_{14}H_{10})$ and $C_{70}(C_5H_6)$. Separation for the fullerene derivatives was conducted by multistep HPLC alternately on four HPLC columns (pyrenebutyric acid, 5PYE, 5PBB, and Buckyprep). The HPLC running procedures are described in the Supporting Information in detail. C_{70}-$(C_{14}H_{10})$ and $C_{70}(C_5H_6)$ show the retention time of 7.5 min in a Buckyprep column (i.d. = 10 × 250 mm, eluted using toluene at a flow rate of 4.0 mL/min) and 25.9 min in a 5PBB column (i.d. = 10 × 250 mm, eluted using toluene at a flow rate of

3.0 mL/min), respectively (Figures S1 and S2, Supporting Information).

2.3. Characterization of $C_{70}(C_{14}H_{10})$ and $C_{70}(C_5H_6)$. MS and MS/MS experiments were performed on a Bruker HCT mass spectrometer interfaced by an atmospheric pressure chemical ionization (APCI). Proton and ^{13}C NMR experiments of C_{70}-$(C_{14}H_{10})$ were carried out on a Bruker AV 400 MHz NMR spectrometer, and the other NMR experiments, such as 2D NMR experiments, were carried out on a Bruker AV 600 MHz NMR spectrometer. FT-IR spectra were measured by a Nicolet Avatar 330 FT-IR spectrometer, and the UV/vis data were collected on a Varian CARY-300 spectrometer.

2.4. Computational Methods. Density functional theory (DFT) calculations were performed using the hybrid density functional B3LYP as implemented in Gaussian 09.[39-42] The standard 6-31G** basis sets were used for C and H atoms. No constraint of freedom was introduced in geometry optimizations of possible isomers of $C_{70}(C_{14}H_{10})$ and $C_{70}(C_5H_6)$. NMR chemical shielding tensors were computed using the GIAO method[42] at the B3LYP/6-31G** theoretical level.

3. RESULTS AND DISCUSSION

3.1. Structural Identification of $C_{70}(C_{14}H_{10})$ and $C_{70}(C_5H_6)$. The APCI source allows the sample to evaporate at an adjustable temperature for ionization. APCI-MS spectra analyzed at the ionization temperature lower than 150 °C show the molecular ion peaks of the isolated $C_{70}(C_{14}H_{10})$ and $C_{70}(C_5H_6)$ at ~1018 and ~906 m/z, respectively (Figure 2). At the temperature of 220 °C, the intensities of C_{70} ions are comparable with the original molecular ions of $C_{70}(C_{14}H_{10})$ or $C_{70}(C_5H_6)$. Increasing the temperature up to 300 °C results in predominate peaks of ~840 m/z in the mass spectra, indicating that $C_{70}(C_{14}H_{10})$ and $C_{70}(C_5H_6)$ are exohedral derivatives of C_{70} subject to pyrolysis to lose their $C_{14}H_{10}$ and C_5H_6 adduct groups.

Note that D_{5h}-symmetric C_{70}, the most stable isomer of the 70-atom carbon cages, turns out to be one of the most abundant fullerenic species in combustion soot.[3-8] The olivary D_{5h}-C_{70} has eight types of nonequivalent C—C bonds (Figure 3). Among them, the [6,6] junctions a—b and c—c are the shortest and always exhibit chemical reactivity of a C=C double bond,[43-46] for example, subject to cycloadditions.[47] On the contrary, those bonds in the equatorial [5]cycloparaphenylene belt are benzene-like and far less reactive.[48] Moreover, it has been shown that the a—b bond is the most reactive in cycloaddition reactions due to its higher π-orbital pyramidalization.[44] Conceivably, the
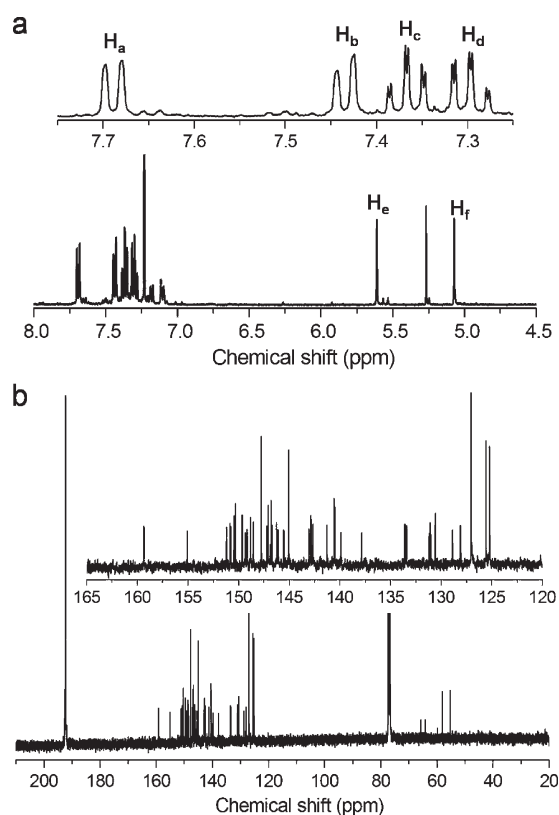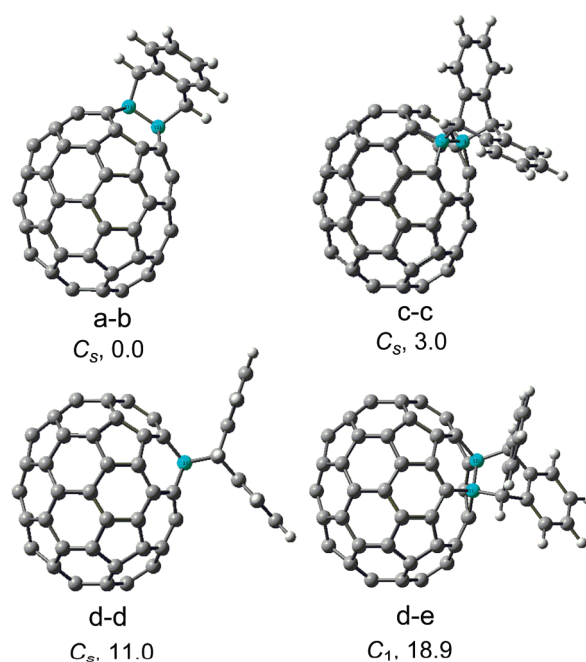
Figure 4. (a) ^{1}H NMR spectrum of $C_{70}(C_{14}H_{10})$ in CS_2/CDCl$_3$. The 5.28 ppm signal is caused by the impurity of CS_2 (see Figure S3 in the Supporting Information), and the multiplet at 7.16 ppm is caused by the residual toluene. The inset is the enlarged downfield portion. (b) ^{13}C NMR spectrum of $C_{70}(C_{14}H_{10})$ with the amplified sp^2 area inserted.
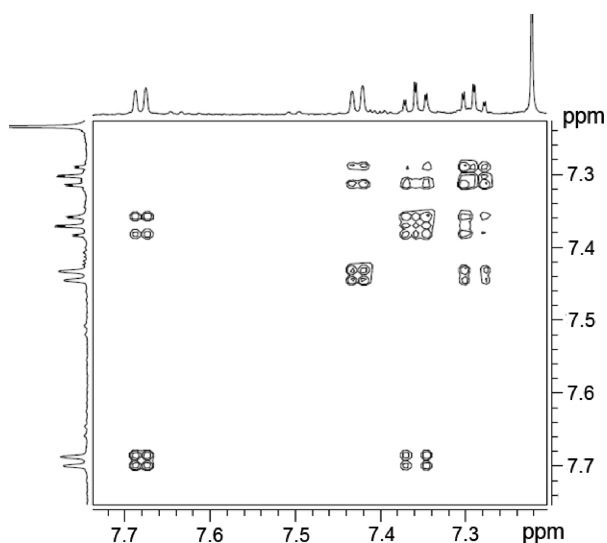
Figure 5. ^{1}H$-^1$H COSY spectrum of $C_{70}(C_{14}H_{10})$.

$C_{70}(C_{14}H_{10})$ and $C_{70}(C_5H_6)$ isolated from the flame soot are most likely formed by Diels−Alder cycloadditions of the diene-like unsaturated cyclic hydrocarbons $C_{14}H_{10}$[49] and C_5H_6, which themselves are combustion products, to the a−b bond of D_{5h}-C_{70}.


Figure 6. Ball-and-stick models of four $C_{70}(C_{14}H_{10})$ adducts on ring junctions (green-colored) with C=C properties. B3LYP/6-31G**-predicted relative energies (in kcal/mol) are given in black numbers.

Figure 4a shows the ^{1}H NMR spectrum of $C_{70}(C_{14}H_{10})$, in which the chemical shifts ranging from 7.3 to 7.7 ppm, that is, H$_a$ (d, 7.69), H$_b$ (d, 7.43), H$_c$ (m, 7.37), and H$_d$ (m, 7.30), are assignable to the protons linking to aryl carbon atoms. The ^{1}H$-^1$H COSY spectrum (Figure 5) reveals the detailed spin−spin coupling correlations among these protons: H$_a \sim$ H$_c$ (J = 7.2 Hz), H$_c \sim$ H$_d$ (J = 7.5 Hz), and H$_b \sim$ H$_d$ (J = 7.3 Hz). Further splits of H$_c$ and H$_d$ are caused by the protons of the *meta*-position carbons (J_{bc} = 1.3 Hz, J_{ad} = 1.4 Hz). H$_e$ (s, 5.61) and H$_f$ (s, 5.07) are assigned to the protons of the bridgehead carbon atoms of $C_{14}H_{10}$. Integral ratios of all protons are nearly 2:2:2:2:1:1. Thus, an anthracene-like fragment can be identified from its ^{1}H NMR and COSY spectra. ^{13}C NMR of $C_{70}(C_{14}H_{10})$ shows a total of 45 peaks with 41 locating in downfield and 4 in upfield. Downfield peaks (ranging from 125.2 to 159.4 ppm) are ascribed to the sp^2-hybridized carbons, whereas the remaining four upfield peaks (55.4, 58.1, 64.1, and 65.8 ppm) result from the sp^3-hyridized carbons (Figure 4b). The ^{1}H and ^{13}C NMR spectra jointly indicate that the $C_{70}(C_{14}H_{10})$ molecule has the C_s symmetry with four unique sp^3-hybridized carbons; that is, the butterfly-like $C_{14}H_{10}$ adduct is added to the a−b bond of D_{5h}-C_{70}.

Density functional theory (DFT) calculations at the B3LYP/6-31G** level of theory were performed for possible cycloaddition products of $C_{14}H_{10}$ to the a−b, c−c, d−d, and d−e sites of D_{5h}-C_{70}. As shown in Figure 6, the $C_{70}(C_{14}H_{10})$ structure with anthracene $C_{14}H_{10}$ attached to the a−b site appears to be the most stable and, meanwhile, renders simulated ^{1}H and ^{13}C NMR spectra (by the GIAO method) agreeing well with the measured spectra (see Figure S5 in the Supporting Information). These theoretical data corroborate the structural identification of $C_{70}(C_{14}H_{10})$, named as 9′,10′-didydro([9,10]ethanoanthra)[11′,12′:8,25] $(C_{70}$-$D_{5h(6)})$[5,6]fullerene according to IUPAC nomenclature.

Similarly, the structure of $C_{70}(C_5H_6)$ can be identified by NMR spectrometry and DFT calculations. The ^{1}H NMR spectrum of

a

b
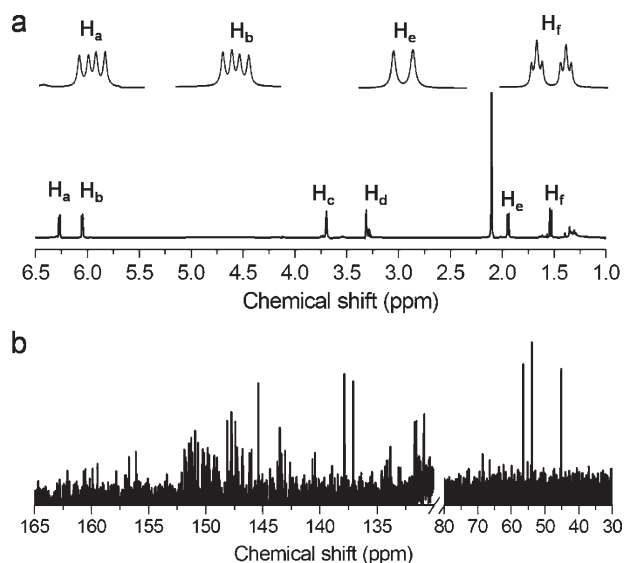
**Figure 7.** (a) ^{1}H NMR spectrum of $C_{70}(C_5H_6)$ in C_6D_6; the inserts are the enlarged signals of H_a, H_b, H_e, and H_f. (b) ^{13}C NMR spectrum of $C_{70}(C_5H_6)$.
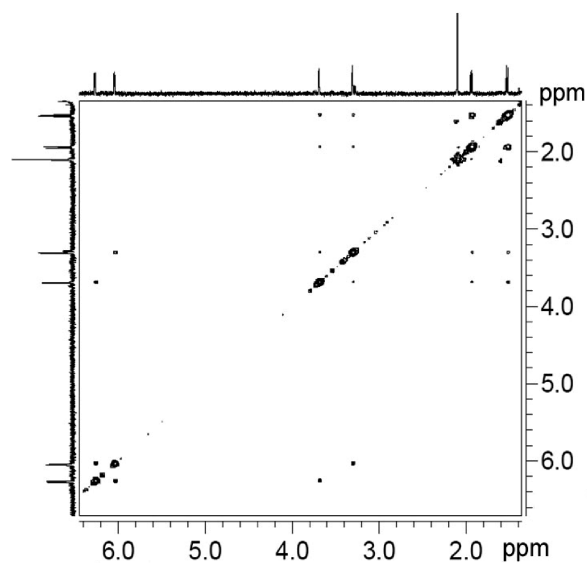
Figure 8. ^{1}H$-$^{1}H COSY spectrum of $C_{70}(C_5H_6)$.

$C_{70}(C_5H_6)$ in C_6D_6 is depicted in Figure 7a, showing a total of six unique H atoms. Their chemical shifts are the following: H_a (q, 6.27, J = 5.7, 3.1 Hz), H_b (q, 6.05, J = 5.7, 3.1 Hz), H_c (s, 3.70), H_d (s, 3.31), H_e (d, 1.94, J = -9.8 Hz), and H_f (m, 1.53, J = -9.7 Hz). The peak-area integral ratios are approximately 1:1:1:1:1:1. Eight H$-$H correlations can be clarified from the COSY spectrum (Figure 8). Further splits (triplet splits of the doublet peaks, J = 1.8 Hz) of H_f in upfield are caused by the weak coupling with two H atoms of the bridgehead. Five upfield signals (45.2, 53.9, 56.5, 66.4, and 68.6 ppm) corresponding to sp^3-hybridized carbon atoms are shown in the ^{13}C NMR spectrum (Figure 7b). In combination with the ^{1}H$-$^{13}C HSQC spectrum (Figure S4, Supporting Information), three of them (45.2, 53.9, and 56.5 ppm) are ascribable to sp^3-hybridized carbon atoms of the cyclopentene portion and the other two peaks (66.4 and 68.6 ppm) are
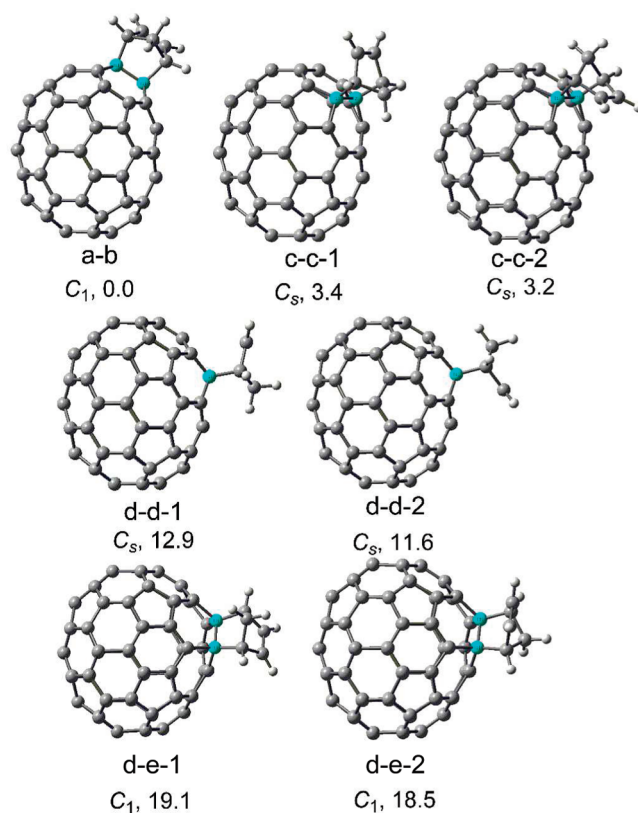
Figure 9. Ball-and-stick models of seven $C_{70}(C_5H_6)$ adducts on ring junctions (green-colored) of a partial C$=$C nature. B3LYP/6-31G**-predicted relative energies (in kcal/mol) are given in black numbers.

assignable to the sp^3-hybridized bridgehead carbon atoms of the D_{5h}-C_{70} cage. The sp^2-hybridized carbon atoms of C_5H_6 show enhanced signals located at 137.1 and 137.9 ppm, in comparison to the other C_{70} sp^2-hybridized carbon atoms ranging from 130.9 to 162.1 ppm. Both the ^{1}H and the ^{13}C NMR spectra indicate that the molecule is in C_1 symmetry with the C_5H_6 moiety attached to the a$-$b site of C_{70}, similar to the case of $C_{70}(C_{14}H_{10})$.

Figure 9 shows the B3LYP/6-31G**-optimized structures for possible cycloaddition products of cyclopentadiene C_5H_6 to different C$-$C bonds of C_{70}. Among them, the C_1-symmetric structure with C_5H_6 attached to the a$-$b site of C_{70} is thermodynamically the most favorable. The calculated ^{1}H and ^{13}C NMR data for this structure agree well with the experimental NMR data (see the Supporting Information). According to the nomenclature of IUPAC, the identified $C_{70}(C_5H_6)$ is named as bicyclo-[2.2.1]hept[2]eno[5',6':8,25] $(C_{70}$-$D_{5h(6)})[5,6]$fullerene.

Of interest is the regioselectivity in both $C_{70}(C_{14}H_{10})$ and $C_{70}(C_5H_6)$ at the a$-$b site. This [6,6] site at the top of the olivary D_{5h}-C_{70} is also the most reactive site ready for derivatization by a traditional chemical method, for example, in the cases of the chemical synthesis of $C_{71}H_2$ and $C_{70}(C_5H_6)$,[50,51] with an implication that the combustion method may be an alternative approach toward fullerene cycloadducts with high regioselectivity.

3.2. IR and UV/vis Spectra of $C_{70}(C_{14}H_{10})$ and $C_{70}(C_5H_6)$. The distinct C$-$H stretching vibration absorptions of C_{70}-$(C_{14}H_{10})$ and $C_{70}(C_5H_6)$ are fairly weak. Both of them are around 2920$-$2845 cm^{-1}, as shown in Figure 10. Other relatively intense absorptions in the fingerprint zone are caused by
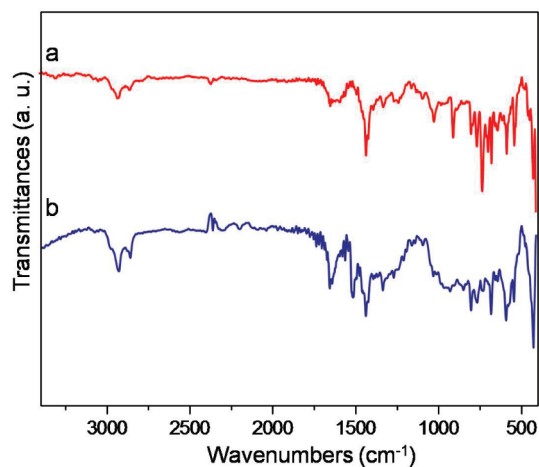
Figure 10. IR spectra of $C_{70}(C_{14}H_{10})$ (a) and $C_{70}(C_5H_6)$ (b).
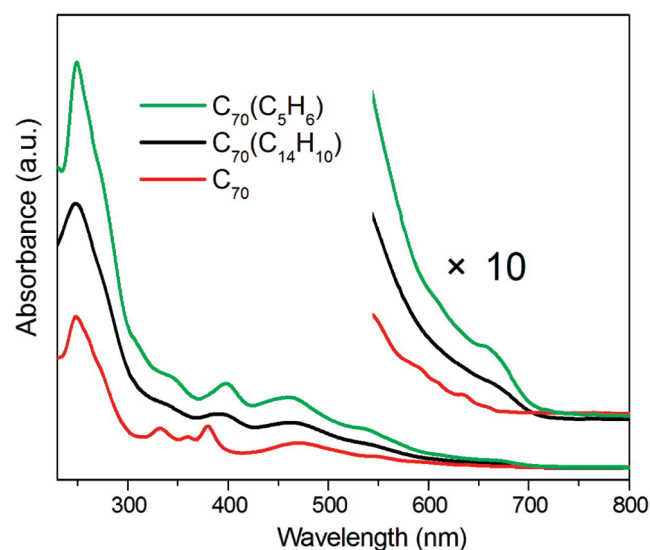

Figure 11. UV/vis spectra of $C_{70}(C_{14}H_{10})$ and $C_{70}(C_5H_6)$ in chloroform solution.

the δ_{C-H}, ν_{C-C}, and skeleton vibrations of both the exohedral portion and the C_{70} cage.

UV/vis spectra show absorptions at 249, 262, 274, 310, 344, 383, 396, 462, and 540 nm for $C_{70}(C_5H_6)$ and the absorptions at 247, 272, 310, 334, 380, 398, 463, and 541 nm for $C_{70}(C_{14}H_{10})$. Both of them are essentially similar to D_{5h}-C_{70} (247, 261, 331, 359, 379, 468, and 541 nm) (Figure 11). The onsets of $C_{70}(C_{14}H_{10})$ and $C_{70}(C_5H_6)$ are 711 and 710 nm, respectively, nearly red shifting for 45 nm compared with D_{5h}-C_{70}, which indicates that the corresponding HOMO−LUMO gaps of $C_{70}(C_5H_6)$ and $C_{70}(C_{14}H_{10})$ are wider than that of D_{5h}-C_{70}.[52]

3.3. Implications of the Flame-Produced C_{70} Derivatives. Numerous previous studies have demonstrated that fullerenes can be produced at high temperature with moderate yields in either premixed or diffused combustions.[3−8,38,53,54] For a diffusion flame with low-pressure benzene/argon/oxygen, the existence of fullerenes was confirmed and the morphologies of soot particles were identified to have a correlation with fullerene formation.[53] Recently, we also reported the preparation of fullerenes

with fused pentagons by a low-pressure acetylene/benzene/oxygen diffusion flame.[38,54] It is almost certain that the flame-produced bare fullerene C_{70} grows by itself at higher temperature and sequentially reacts with $C_{14}H_{10}$ and C_5H_6 at lower temperature. During the combustion process, therefore, C_{70} can serve as a "sponge" to catch smaller radicals or molecules, for example, anthracene $C_{14}H_{10}$ and cyclopentadiene C_5H_6. In addition to $C_{70}(C_{14}H_{10})$ and $C_{70}(C_5H_6)$, a variety of other fullerene derivatives, such as $C_{61}H_2$, $C_{71}H_2$, $C_{60}(C_{14}H_{10})$, and $C_{76}(C_5H_6)$, are detectable also. Note that we can only exemplify a few derivatives in this manner.

Polycyclic aromatic hydrocarbons (PAHs) are considered as the "building blocks" for further generation of fullerenes and soot in the flames. Siegmann and co-workers designed a gas-inlet system coupled with a time-of-flight mass spectrometer for studying the relationship between fullerene and the PAHs (up to $C_{64}H_{20}$) produced at different heights of an atmospheric methane/oxygen diffusion flame.[55,56] Howard and co-workers suggested that the curved and planar PAHs, subject to competition in the growth process involving C_2H_2 addition, were responsible for the formations of fullerenes and soot, respectively. They proposed that the continued incorporation of C_5 rings would lead to the curvature in PAHs and finally result in a closed cage with 12 C_5 rings.[25] Nevertheless, Homann and co-workers emphasized an important role involving bimolecular reactions between two PAHs for fullerene growth, that is, the so-called "zipper mechanism".[24] On the basis of this mechanism, curved PAHs are not necessary in the bimolecular reactions toward fullerenes. It is not unreasonable for PAHs to form the needed 12 C_5 rings at the brim concerted through hydrogen elimination. Finally, all the pentagons are optimized to the most energetically favorable positions by intramolecular rearrangement within the nascent fullerene to form the most stable isomer. In the present work, the isolation and identification of $C_{70}(C_{14}H_{10})$ and $C_{70}(C_5H_6)$ implies the prevalence of $C_{14}H_{10}$ and C_5H_6 in the flame. In the literature, these species have been predicted as the intermediates leading to fullerene and soot.[22,26] Indeed, the pentagonal framework of C_5H_6 is the key unit for further growth of curved PAHs, which facilitates fullerene formation by incorporation of more C_5 rings during Howard's growth process. On the other hand, the hexagonal skeleton of $C_{14}H_{10}$ is the basic building block of planar PAHs, which are the precursors of large soot particles, or undergoes a "zipper mechanism", leading to entirely closed cages. Therefore, the present work may provide a practical method to capture the possible intermediates and to explore the mechanism responsible for fullerene or soot particle formation in the combustion process. However, more powerful evidence should be obtained to elucidate the authentic mechanism, and further theoretical and experimental studies are now opened.

4. SUMMARY

Two exohedral C_{70} derivatives, $C_{70}(C_{14}H_{10})$ and $C_{70}(C_5H_6)$, have been isolated from the soot of the acetylene−benzene combustion. MS, NMR, IR, and UV/vis spectra in combination with DFT calculations showed that they are actually Diels−Alder adducts of anthracene and cyclopentadiene to the polar a−b site of the olive-shaped D_{5h}-C_{70}. The groups of C_5H_6 and $C_{14}H_{10}$ are considered as the possible intermediates toward larger fullerenes or soot particles but are captured by the in situ formed C_{70} to survive as $C_{70}(C_{14}H_{10})$ and $C_{70}(C_5H_6)$. This work implies that

the combustion method may be an alternative approach to fullerene cycloadducts with high regioselectivity and, on the other hand, demonstrates that C_{70} derivatives are isolatable and informative for mechanistic study. Starting from this work, separation and characterization of more fullerene derivatives in flame might be envisaged.

■ ASSOCIATED CONTENT

ⓢ Supporting Information. HPLC separations of C_{70}-$(C_{14}H_{10})$ and $C_{70}(C_5H_6)$, ^{1}H NMR of CS_2/$CDCl_3$ background, HSQC spectrum of $C_{70}(C_5H_6)$, theoretical computations of NMR data, and Cartesian coordinates of DFT-optimized C_{70}-(C_5H_6) and $C_{70}(C_{14}H_{10})$ structures. This material is available free of charge via the Internet at http://pubs.acs.org.

■ AUTHOR INFORMATION

Corresponding Author
*Fax: (+86)-592-2183047. E-mail: syxie@xmu.edu.cn (S.-Y.X.), xinlu@xmu.edu.cn (X.L.).

■ ACKNOWLEDGMENT

■ REFERENCES

(1) Krätschmer, W.; Lamb, L. D.; Fostiropoulos, K.; Huffman, D. R. *Nature* **1990**, *347*, 354.

(2) Krätschmer, W.; Fostiropoulos, K.; Huffman, D. R. *Chem. Phys. Lett.* **1990**, *170*, 167.

(3) Gerhardt, P.; Löffler, S.; Homann, K.-H. *Chem. Phys. Lett.* **1987**, *137*, 306.

(4) Howard, J. B.; Mckinnon, J. T.; Makarovsky, Y.; Lafleur, A. L.; Johnson, M. E. *Nature* **1991**, *352*, 139.

(5) Howard, J. B.; McKinnon, J. T.; Johnson, M. E.; Makarovsky, Y.; Lafleur, A. L. *J. Phys. Chem.* **1992**, *96*, 6657.

(6) Richter, H.; Labrocca, A. J.; Grieco, W. J.; Taghizadeh, K.; Lafleur, A. L.; Howard, J. B. *J. Phys. Chem. B* **1997**, *101*, 1556.

(7) Goel, A.; Hebgen, P.; Vander Sande, J. B.; Howard, J. B. *Carbon* **2002**, *40*, 177.

(8) Takehara, H.; Fujiwara, M.; Arikawa, M.; Diener, M. D.; Alford, J. M. *Carbon* **2005**, *43*, 311.

(9) Taylor, R.; Langley, G. J.; Kroto, H. W.; Walton, D. R. M. *Nature* **1993**, *366*, 728.

(10) Crowley, C.; Kroto, H. W.; Taylor, R.; Walton, D. R. M.; Bratcher, M. S.; Cheng, P. C.; Scott, L. T. *Tetrahedron Lett.* **1995**, *36*, 9215.

(11) Crowley, C.; Taylor, R.; Kroto, H. W.; Walton, D. R. M.; Cheng, P. C.; Scott, L. T. *Synth. Met.* **1996**, *77*, 17.

(12) Conley, N. R.; Lagowski, J. J. *Carbon* **2002**, *40*, 949.

(13) Xie, S. Y.; Huang, R. B.; Yu, L. J.; Ding, J.; Zheng, L. S. *Appl. Phys. Lett.* **1999**, *75*, 2764.

(14) Xie, S. Y.; Deng, S. L.; Huang, R. B.; Yu, L. J.; Zheng, L. S. *Chem. Phys. Lett.* **2001**, *343*, 458.

(15) Kroto, H. W.; Health, J. R.; O'Brien, S. C.; Curl, R. F.; Smalley, R. E. *Nature* **1985**, *318*, 162.

(16) Xie, S. Y.; Huang, R. B.; Chen, L. H.; Huang, W. J.; Zheng, L. S. *Chem. Commun.* **1998**, 2045.

(17) Xie, S. Y.; Huang, R. B.; Deng, S. L.; Yu, L. J.; Zheng, L. S. *J. Phys. Chem. B* **2001**, *105*, 1734.

(18) Boorum, M. M.; Vasil'ev, Y. V.; Drewello, T.; Scott, L. T. *Science* **2001**, *294*, 828.

(19) Scott, L. T.; Boorum, M. M.; McMahon, B. J.; Hagen, S.; Mack, J.; Blank, J.; Wegner, H.; de Meijere, A. *Science* **2002**, *295*, 1500.

(20) Scott, L. T. *Angew. Chem., Int. Ed.* **2004**, *43*, 4994.

(21) Jackson, E. A.; Steinberg, B. D.; Bancu, M.; Wakamiya, A.; Scott, L. T. *J. Am. Chem. Soc.* **2007**, *129*, 484.

(22) Pope, C. J.; Marr, J. A.; Howard, J. B. *J. Phys. Chem.* **1993**, *97*, 11001.

(23) Pope, C. J.; Howard, J. B. *Tetrahedron* **1996**, *52*, 5161.

(24) Homann, K.-H. *Angew. Chem., Int. Ed.* **1998**, *37*, 2434.

(25) Richter, H.; Howard, J. B. *Prog. Energy Combust. Sci.* **2000**, *26*, 565 and references cited therein.

(26) Richter, H.; Howard, J. B. *Phys. Chem. Chem. Phys.* **2002**, *4*, 2038.

(27) Smyth, K. C.; Crosley, D. R. *Detection of Minor Species with Laser Techniques*; Kohse-Höinghaus, K., Jeffries, J. B., Eds.; Taylor & Francis: New York, 2002; p 9.

(28) Dreier, T.; Ewart, P. *Coherent Techniques for Measurements with Intermediate Concentrations*; Kohse-Höinghaus, K., Jeffries, J. B., Eds.; Taylor & Francis: New York, 2002; p 69.

(29) Lazzara, C. P.; Biordi, J. C.; Papp, J. F. *Combust. Flame* **1973**, *21*, 371.

(30) Cool, T. A.; Nakajima, K.; Mostefaoui, T. A.; Qi, F.; Mcllroy, A.; Westmoreland, P. R.; Law, M. E.; Poisson, L.; Peterka, D. S.; Ahmed, M. *J. Chem. Phys.* **2003**, *119*, 8356.

(31) McEnally, C. S.; Pfefferle, L. D.; Atakan, B.; Kohse-Höinghaus, K. *Prog. Energy Combust. Sci.* **2006**, *32*, 247.

(32) Li, Y. Y.; Qi, F. *Acc. Chem. Res.* **2010**, *43*, 68.

(33) Hirsch, A.; Brettreich, M. *Fullerenes: Chemistry and Reactions*; Wiley-VCH: Weinheim, 2004 and references cited therein.

(34) Krusic, P. J.; Wasserman, E.; Keizer, P. N.; Morton, J. R.; Preston, K. F. *Science* **1991**, *254*, 1183.

(35) Chiang, L. Y. U.S. Patent 5,648,523, 1997.

(36) Zeynalov, E. B.; Allen, N. S.; Salmanova, N. I. *Polym. Degrad. Stab.* **2009**, *94*, 1183.

(37) Rotello, V.; Howard, J. B.; Yadava, T.; Conna, M.; Viania, E.; Giovanea, L.; Lafleur, A. *Tetrahedron Lett.* **1993**, *34*, 1561.

(38) Weng, Q. H.; He, Q.; Liu, T.; Huang, H. Y.; Gao, Z. Y.; Chen, J. H.; Xie, S. Y.; Lu, X.; Huang, R. B.; Zheng, L. S. *J. Am. Chem. Soc.* **2010**, *132*, 15093. For the detailed description and scheme of our homemade combustion apparatus, please see the Supporting Information therein.

(39) Lee, C.; Yang, W.; Parr, R. G. *Phys. Rev. B* **1988**, *37*, 785.

(40) Wolinski, K.; Hilton, J. F.; Pulay, P. J. *J. Am. Chem. Soc.* **1990**, *112*, 8251 and references cited therein.

(41) Becke, A. D. *J. Chem. Phys.* **1993**, *98*, 5648.

(42) The GIAO-B3LYP calculations were performed with the Gaussian 09 A.02 suite of programs: Frisch, M. J.; et al. *Gaussian 09*, rev. A.02; Gaussian, Inc.: Wallingford, CT, 2009.

(43) Taylor, R.; Hare, J. P.; Abkul-Sada, A. K.; Kroto, H. W. *J. Chem. Soc., Chem. Commun.* **1990**, 1423.

(44) Haddon, R. C. *Science* **1993**, *261*, 1545.

(45) Taylor, R. *J. Chem. Soc., Perkins Trans. 2* **1993**, 813.

(46) Bürgi, H. B.; Venugopalan, P.; Schwarzenbach, D.; Diederich, F.; Thilgen, C. *Helv. Chim. Acta* **1993**, *76*, 2155.

(47) Segura, J. L.; Martin, N. *Chem. Rev.* **1999**, *99*, 3199 and references therein.

(48) Li, B.; Shu, C. Y.; Lu, X.; Dunsch, L.; Chen, Z. F.; Dennis, T. J. S.; Shi, Z. Q.; Jiang, L.; Wang, T. S.; Xu, W.; Wang, C. R. *Angew. Chem., Int. Ed.* **2010**, *49*, 962.

(49) Wang, G. W.; Saunders, M.; Cross, R. J. *J. Am. Chem. Soc.* **2001**, *123*, 256.

(50) Smith, A. B., III; Strongin, R. M.; Brard, L.; Furst, G. T.; Romanow, W. J.; Owens, K. G.; Goldschmidt, R. J.; King, R. C. *J. Am. Chem. Soc.* **1995**, *117*, 5492.

(51) Pang, L. S. K.; Michael, A. W. *J. Phys. Chem.* **1993**, *97*, 6761.

(52) Li, J.; Feng, J. K.; Sun, C. C. *Int. J. Quantum Chem.* **1994**, *52*, 673.

(53) Hebgen, P.; Goel, A.; Howard, J. B.; Rainey, L. C.; van der Sande, J. B. *Proc. Combust. Inst.* **2000**, *28*, 1397.

(54) Gao, Z. Y.; Jiang, W. S.; Sun, D.; Xie, S. Y.; Huang, R. B.; Zheng, L. S. *Combust. Flame* **2010**, *157*, 966.

(55) Siegmann, K.; Hepp, H.; Sattler, K. *Surf. Rev. Lett.* **1996**, *3*, 741.

(56) Siegmann, K.; Sattler, K. *J. Chem. Phys.* **2000**, *112*, 698.